First-principles analysis of electronic states in silicon nanoscale quantum wires

Mark S. Hybertsen and Mark Needels*
AT&T Bell Laboratories, 600 Mountain Avenue, Murray Hill, New Jersey 07974
(Received 4 January 1993; revised manuscript received 19 February 1993)

The atomic structure of small-cross-section (≈ 10 Å), hydrogen-terminated silicon quantum wires is fully relaxed within the local-density approach showing bulklike coordination of the Si atoms. The electronic states near the fundamental gap (substantially blueshifted from that of bulk Si) show a direct gap between bulk-Si-derived states. The new dipole matrix elements and the detailed level orderings depend on the size, symmetry, and surface structure of the wire. The optical response is presented with the implications of the valley orbit splitting for radiative dynamics in light-emitting porous silicon.

The report of bright luminescence from anodically etched Si wafers ("porous Si") (Ref. 1) has renewed interest in the subject of light emission from "engineered" structures based on Si. Normally, photoluminescence from bulk Si is quite weak due to the indirect fundamental gap. The relatively strong signal from porous Si samples, together with the substantial blueshift of the radiation, naturally suggests that the luminescence arises from some type of nanostructure in the sample e.g., small quantum wires.[2,3] Although this may be an idealization, it has focused attention on the optical properties of Si microcrystallites.[4]

In this paper, we study a class of idealized Si quantum wires. The first-principles approach, based on the self-consistent local-density approximation (LDA), allows us to study nanostructures which have (meta)stable atomic positions and to obtain the full electronic structure. The hydrogen terminated wires, although of small diameter (≈ 10 Å), reveal a number of interesting features. The fundamental gap is direct and involves states of predominantly bulk Si character. The lowest transitions are dipole allowed with matrix elements induced due to confinement. This microscopic result supports a more general analysis based on envelope-function considerations,[5,6] as do related studies based on a tight-binding approach,[7,8] and agrees with other LDA calculations.[9] Even these ideal structures have a rich electronic structure: the detailed valley-orbit splitting and ordering depends on the symmetry of the wire as well as the structure in the surface region. The dipole matrix elements vary by more than an order of magnitude among the various low-energy interband transitions in a given wire, with interesting consequences for the optical properties and implications relevant to light-emitting porous Si.

The wires studied extend along the [001] direction with the exposed (110) faces terminated by the hydrogen atoms (Fig. 1). We consider a 5×5 wire ($Si_{25}H_{20}$ per unit cell) of $P\bar{4}m2$ symmetry and a 5×6 wire ($Si_{30}H_{22}$ per unit cell) with the lower $P2/m$ symmetry. The atomic structure has been optimized to minimize the total energy using a steepest-descent algorithm applied to both the electronic and atomic degrees of freedom within the LDA.[10] The electronic structure calculation is performed using a plane-wave basis (12-Ry cutoff). The Si ions are represented by a norm-conserving, separable, nonlocal pseudopotential while the bare Coulomb interaction is used for the H ions. The one-dimensional Brillouin zone along the wire axis is sampled by two points. There is negligible coupling between wires which form a two-dimensional periodic array with lattice spacing $2\sqrt{2}a_{\text{bulk}}$. The resulting atomic structure still shows closely tetrahedral bonding with Si-H bond-angle deviations of ± 1–$2°$. The Si-H bond length is about 4–5% longer than found in SiH_4, while the Si-Si bond lengths only vary by 0.01 Å. These structures represent rather ideal crystalline Si quantum wires.

The band structure of the 5×5 wire is shown in Fig. 2. The bands are aligned to the bulk-Si-projected band structure and have been approximately corrected [11] for the self-energy effects which are necessary for the correct band gap.[12] The quantum-wire bands are clearly pulled away from the bulk band edges by the kinetic energy of confinement. The bands with the most Si-H character are several eV from the band edges, with a Si-H bonding

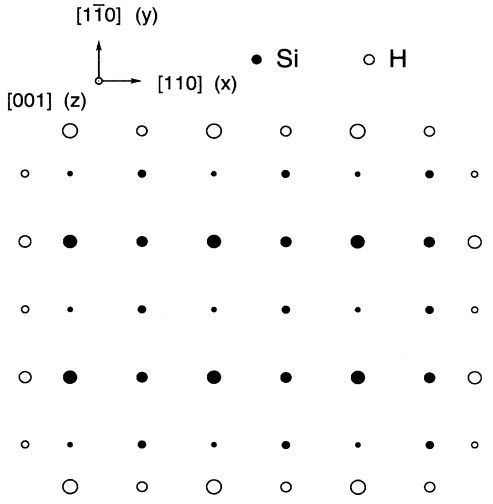

FIG. 1. One unit cell (four layers) of the quantum wires studied. The size of the circle increases with height. There are $M\times N$ Si atoms per cell, e.g., 6×5 here.

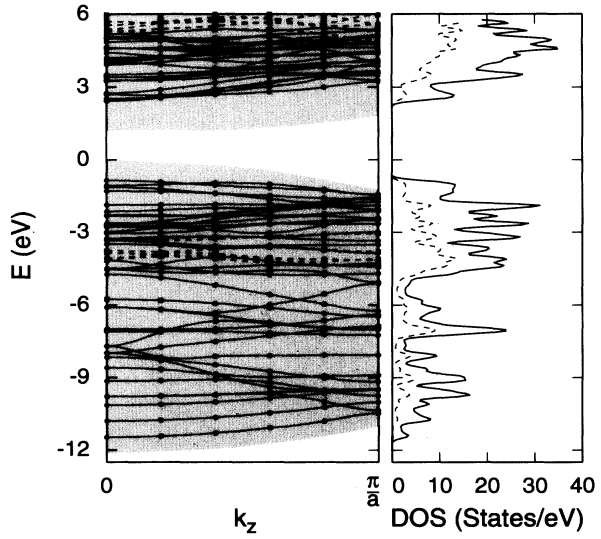

FIG. 2. The band structure of the 5×5 wire together with the projected bulk energy bands of Si (gray) plotted vs wave vector along the wire and the associated density of states (solid curve at right with Gaussian burdening of 0.1 eV). The dashed lines indicate bands with more than 50% Si-H character. The Si-H projected density of states (dashed curve at right) is defined so as to include two electrons per Si-H bond.

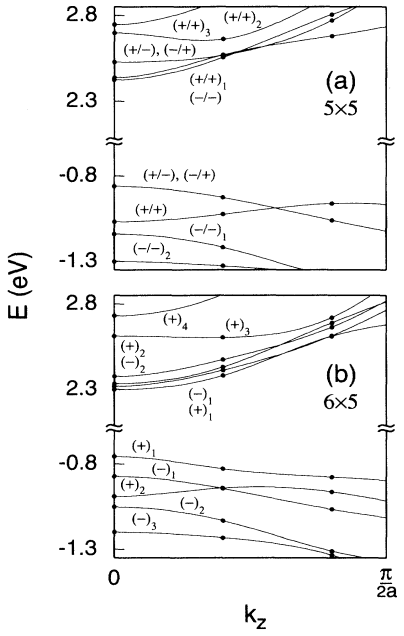

FIG. 3. A detailed view of the 5×5 (a) and 6×5 (b) wire band structure near the region of the fundamental gap. Note the broken energy scale. The bands are labeled by symmetry (see text).

to antibonding separation of 8–10 eV. However, because there are no extra gaps in the bulk projected bands, these states are of necessity resonances rather than fully localized surface states. This is clear in the density of states which shows Si-H character spread over the entire spectral range.

The states nearest the band edge are shown in Fig. 3 for both the 5×5 and 6×5 cases. The states in the 5×5 wire are classified according to the (x/y) mirror planes, with the $(+/-)$ and $(-/+)$ states degenerate [neglecting the small spin-orbit interaction in Si (Ref. 7)], while in the 6×5 wire only the (x) mirror plane can be used. The main feature of the valence-band states is the splitting at the zone center. The lowest four conduction bands derive from the $\Delta_{x,y}$ valleys, while the next two come from the Δ_z valleys. The latter are higher since the lighter (transverse) mass of the Δ_z valleys controls the kinetic energy of confinement. These valleys also have a larger weight in the Si-H barrier region. The valleys are further split by valley-orbit interaction due to the potential at the surface.

The level ordering and spacing is sensitive to the Si-H barrier potential. The lowest four conduction bands for the 5×5 wire, calculated in the local-density approximation for the relaxed structure, are 1.64, 1.67, and 1.75 eV (doublet) at $k_z=0$, while the self-energy-corrected values are 2.43, 2.44, and 2.53 eV. The changes in spacing reflect the differing degrees of penetration into the Si-H region. For an ideal structure prior to atomic relaxation, or if the Si-H bond length is uniformly contracted by a few percent, the lower two levels are interchanged and yield a level ordering in agreement with Ohno, Shiraishi, and Ogawa.[9] This further demonstrates the sensitivity of the valley-orbit interaction to the details of the surface potential. The valence-band order is different than suggested by the kinetic energy of confinement calculated in a $\mathbf{k}\cdot\mathbf{p}$ approach. Compared to a tight-binding calculation,[7] the $(+/-)$, $(-/+)$ doublet is reversed relative to the $(+/+)$ and $(-/-)$ states in both the valence and conduction bands. Since the Si-H tight-binding parameters were not explicitly fit to a control molecule, these differences probably trace to the potential in the Si-H region.

The optical properties of the wires are studied by evaluating the absorption coefficient:

$$\alpha_e(\omega)=\frac{4\pi^2e^2}{ncm_e^2\omega V_c}\sum_{v,c,k_z}|\mathbf{e}\cdot\mathbf{p}_{cv}(k_z)|^2\delta(E_{ck_z}-E_{vk_z}-\hbar\omega)\ , \tag{1}$$

where n is the refractive index of the medium, V_c is the unit cell size for the present array of wires, and the transition dipole $\mathbf{p}_{cv}$ is calculated[13] for each polarization $\mathbf{e}$. The density (porosity) of the present array enters through V_c and n (estimated to be ≈ 2.7 and ≈ 2.9 for the 5×5 and 6×5 wires[14]). Excitonic effects are not included. A joint density of states for allowed transitions in the 5×5 wire [Fig. 4(a)] shows a large number of possible transitions due to the valley-orbit splitting. Only a few have sufficient oscillator strength to be appreciable in the absorption cross section [in cm^{-1}, Fig. 4(b)]. Although the onset at about 3.3 eV is relatively weak, there are three strong transitions within 0.3 eV. The 6×5 wire shows a

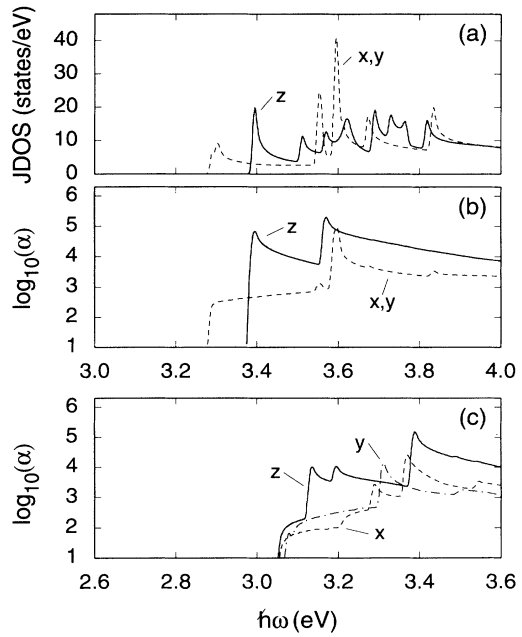

FIG. 4. (a) Joint density of states including only the low-energy dipole-allowed optical transitions of indicated polarization for the 5×5 wire. (b) Log base ten of the absorption cross section (in cm^{-1}) calculated for the array of 5×5 wires (equivalent porosity ≈40–50%, Gaussian broadening of 5 meV). (c) The same for the 6×5 wires (porosity ≈30–40%).

more complex set of transitions [Fig. 4(c)]. The z polarization (along the wire axis) transitions dominate near threshold for both cases. The absorption cross section and threshold are reduced for the wire of larger cross-sectional area, consistent with effective-mass models.[5,6]

The confinement in these narrow wires has induced substantial mixing of the bulk-band-edge-derived states with other states across the Brillouin zone. As a consequence, the low-energy transitions have direct, nonzero dipoles, in contrast to bulk Si, where phonons or defects mediate the absorption or emission of light. Of direct importance to understanding the luminescence of these ideal wires is the associated radiative rate

$$W_{\rm sp}(\omega)=\tfrac{4}{3}n\omega\frac{e^2}{\hbar c}\frac{|\mathbf{p}_{cv}|^2/2m_e}{m_e c^2}\ . \qquad (2)$$

We consider zone-center interband transitions and average over the four possible electron and hole spin configurations. The spontaneous emission time ($\tau_{\rm sp}=1/W_{\rm sp}$) enters the emission rate per unit volume ($R=n_{\rm min}/\tau_{\rm sp}$) controlled by the minority carrier density in the dipole allowed case. The $\tau_{\rm sp}$ are tabulated (Table I) for the lowest-energy transitions, split by the valley-orbit interaction. These radiative times span several orders of magnitude, with the fastest times being of order tens of nanoseconds for these small wires.[15] In the 5×5 wire, the (+/−), (−/+) conduction-band states show the strongest dipole coupling to the valence-band-edge states. This z-polarized coupling derives from the intraband mixing (within the Δ_{5v} band for hole states and the Δ_{1c} band for the electron states). The x,y-polarized coupling for the (+/+) and (−/−) states is much weaker, being due to an interband mixing (Δ_{2c} band for the electron states). This suppresses the radiative rate by two to three orders of magnitude. It also explains the dominance of z polarization in Figs. 4(b) and 4(c). Although these details of the valley-orbit splitting are outside the scope of simple effective-mass models, the intraband mixing treated in the envelope approximation[5,6] is basically correct. The effective-mass theory predicts strongly size-dependent induced dipoles.[5,6] This is consistent with the data in Table I (comparing the fast time for the 5×5 and 6×5 cases) and other LDA calculations.[9]

Excitonic effects are important for effective one-dimensional systems, e.g., the shape, intensity, and positions of the absorption thresholds in Fig. 4 would be altered. However, our key conclusions depend on the underlying band-structure effects. Furthermore, as Read *et al.* note,[9] fluctuations in wire dimension in actual samples will set a length scale for electrons and holes of the order of the excitonic radius. This quenches most of the excitonic enhancement which might enter in Eq. (2).

Our results have qualitative implications for understanding the time and temperature dependence of photoluminescence from porous or microcrystalline Si. We assume that radiative recombination occurs between thermally occupied low-energy electron and hole states. We focus on the radiative dynamics, hypothesizing that nonradiative centers may play a small role due to hydrogen passivation during processing. Several experiments report nonexponential decay of the luminescence intensity.[16–19] The LDA calculations (present and Ref. 9) as well as the effective-mass theory[5,6] exhibit strong size- and symmetry-dependent radiative times. The nonexponential decay could be modeled by an ensemble of active nanostructures. Furthermore, the decay characteristics are observed to be strongly temperature dependent,[17–19] with a large, slow component appearing or being enhanced at low temperature. Our results show that, within a given wire (or active nanostructure), several low-lying excitons exist with widely different radiative times due to valley-orbit splitting effects, as also noted by Ohno, Shiraishi, and Ogawa.[9] The lower-energy excitons

TABLE I. Calculated band-to-band transition energies and spontaneous radiative times for selected low-energy transitions. The valence- and conduction-band states are designated by the symmetry label (Fig. 3).

Transition $v\rightarrow c$	Pol.	E_c-E_v (eV)	$\tau_{\rm sp}$ (s)
	5×5		
$(+/-)\rightarrow(-/-)$	$x(y)$	3.29	8×10^{-6}
$(-/+)\rightarrow(+/+)$	$x(y)$	3.30	4×10^{-5}
$(-/+)\rightarrow(-/+)$	z	3.39	4×10^{-8}
$(+/-)\rightarrow(+/-)$	z	3.39	4×10^{-8}
	6×5		
$(+)_1\rightarrow(-)_1$	y	3.08	2×10^{-5}
$(+)_1\rightarrow(+)_2$	z	3.13	8×10^{-8}

are the slowest. At high temperature, occupation of the higher-energy states will lead to relatively fast decay. However, the fast component will be frozen out at low temperature, leaving most of the recombination in the slow component. The crossover temperature is related to the calculated splitting, which for realistic wire dimensions would probably be about 5–10 times smaller than found here (i.e., scaling with the wire area).

Splitting between singlet and triplet excitons has also been proposed as an explanation for the crossover temperature.[19] We emphasize that the valley-orbit splitting effect is a generic feature of the electronic structure of Si nanostructures, as is the exchange splitting of the corresponding excitons, with similar energy scales for the relevant sizes. For the present wires, e.g., the 5×5 case, the orbital and spin degrees of freedom yield 32 low-lying excitons, the coupling of which through spin-orbit and exchange interactions must be considered to properly analyze the radiative dynamics,[20] as well as magnetic-field effects.[19] In particular, a theory including valley-orbit, spin-orbit, and exchange interactions on an equal footing for low-symmetry structures characteristic of porous Si is desirable.

The multivalley conduction bands in Si lead to a rich low-energy electronic structure for Si quantum wires. The level splitting and order depends on the details of the structure, e.g., local bond lengths. This dependence suggests that the electron-phonon interaction may play an important role in the radiative transitions. Earlier estimates for the efficiency of phonon-mediated transitions raised this point.[5] Recent spectra for porous Si have resolved phonon sidebands.[19] These points further suggest the radiative dynamics of Si nanostructures to be an important open area for further investigation.

---

*Present address: Lawrence Livermore National Laboratory, Livermore, CA.

[1]L. T. Canham, Appl. Phys. Lett. **57**, 1046 (1990).

[2]A. G. Cullis and L. T. Canham, Nature **353**, 335 (1991).

[3]V. Lehmann and U. Gosele, Appl. Phys. Lett. **58**, 856 (1991); A. Halimaoui, C. Oules, G. Bomchil, A. Bsiesy, F. Gaspard, R. Herino, M. Ligeon, and F. Muller, Appl. Phys. Lett. **59**, 304 (1991).

[4]See, e.g., H. Takagi, H. Ogawa, Y. Yamazaki, A. Ishizaki, and T. Nakagiri, Appl. Phys. Lett. **56**, 2379 (1990); K. A. Littau, P. J. Szajowski, A. J. Muller, A. R. Kortan, and L. E. Brus, J. Phys. Chem. **97**, 1224 (1993).

[5]M. S. Hybertsen, in *Light Emission from Silicon,* edited by S. S. Iyer, L. T. Canham, and R. T. Collins (Materials Research Society, Pittsburgh, 1992), p. 179.

[6]M. Yamamoto, R. Hayashi, K. Tsunetomo, K. Kohno, and Y. Osaka, Jpn. J. Appl. Phys. **30**, 136 (1991); T. Takagahara and K. Takeda, Phys. Rev. B **46**, 15 578 (1992).

[7]G. D. Sanders and Y.-C. Chang, Phys. Rev. B **45**, 9202 (1992).

[8]J. R. Proot, C. Delerue, and G. Allan, Appl. Phys. Lett. **61**, 1948 (1992).

[9]A. J. Read, R. J. Needs, K. J. Nash, L. T. Canham, P. D. J. Calcott, and A. Qtiesh, Phys. Rev. Lett. **69**, 1232 (1992); F. Buda, J. Kohanoff, and M. Parrinello, *ibid.* **69**, 1272 (1992); T. Ohno, K. Shiraishi, and T. Ogawa, *ibid.* **69**, 2400 (1992).

[10]M. Needels, J. D. Joannopoulous. Y. Bar-Yam, and S. T. Pantelides, Phys. Rev. B **43**, 4208 (1991).

[11]The bulk Si band gap error is 0.7 eV (Ref. 12). The lowest molecular transition for SiH_4 ($\approx$9.0 eV) [M. B. Robin, *Higher Excited States of Polyatomic Molecules* (Academic, New York, 1974)] exceeds our calculated value by about 1.5 eV. The approximate self-energy correction for the wire states is taken as an average of these according to the Si-H weight, symmetrically applied to the valence and conduction bands. The correction to the minimum gap is 0.88 and 0.84 eV for the 5×5 and 6×5 wires, respectively.

[12]M. S. Hybertsen and S. G. Louie, Phys. Rev. B **34**, 5390 (1986).

[13]Corrections due to the use of nonlocal pseudopotentials, expected to be small, are neglected: A. J. Read and R. J. Needs, Phys. Rev. B **44**, 13 071 (1991).

[14]These correspond to the as-calculated structure, for concreteness. In high-porosity samples, the effective index will be smaller, e.g., approaching $n\approx1$. (Read *et al.*, Ref. 9, cite $n=1.2$.)

[15]The lowest transition at $k=0$ in the 6×5 wires $[(+)_1\rightarrow(+)_1]$ is forbidden, although it acquires a matrix element for finite k showing that the corresponding exciton is weakly allowed with a radiative time which will be slower than $\approx10^{-5}$ s.

[16]J. C. Vial, A. Bsiesy, F. Gaspard, R. Herino, M. Ligeon, F. Muller, R. Romestain, and R. M. Macfarlane, Phys. Rev. B **45**, 14171 (1992).

[17]Y. H. Xie, W. L. Wilson, F. M. Ross, J. A. Mucha, E. A. Fitzgerald, J. M. Macaulay, and T. D. Harris, J. Appl. Phys. **71**, 2403 (1992); W. L. WIlson (private communication).

[18]X. Chen, B. Henderson, and K. P. O'Donnell, Appl. Phys. Lett. **60**, 2672 (1992).

[19]P. D. J. Calcott, K. J. Nash, L. T. Canham, M. J. Kane, and M. D. Brumhead, J. Phys. Condens. Matter **5**, L91 (1993).

[20]M. S. Hybertsen (unpublished).

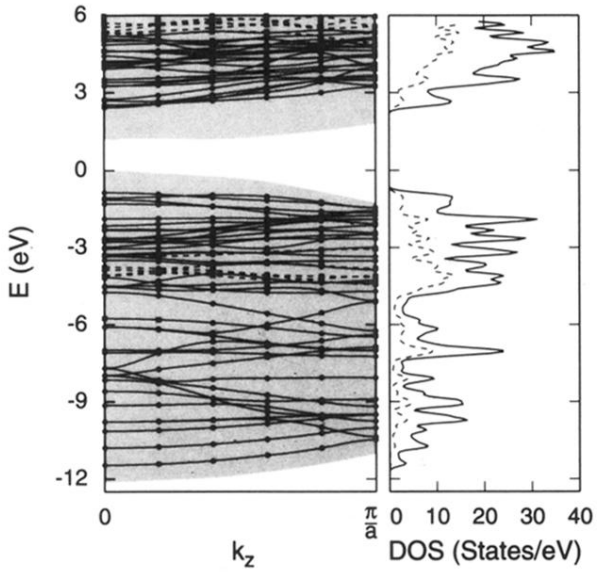

FIG. 2. The band structure of the 5×5 wire together with the projected bulk energy bands of Si (gray) plotted vs wave vector along the wire and the associated density of states (solid curve at right with Gaussian burdening of 0.1 eV). The dashed lines indicate bands with more than 50% Si-H character. The Si-H projected density of states (dashed curve at right) is defined so as to include two electrons per Si-H bond.